Steel and Composite Structures, Vol. 8, No. 6 (2008) 491-510 491
DOI: http://dx.doi.org/10.12989/scs.2008.8.6.491

A Study on the fire-resistance of concrete-filled steel square tube columns without fire protection under constant central axial loads

Su-Hee Park and Sung-Mo Choi*

Department of Architectural Engineering, University of Seoul, Korea

Kyung-Soo Chung

Architectural Engineering Research Team, Research Institute of Industrial Science and Technology, Korea

(Received June 4, 2008, Accepted November 4, 2008)

Abstract. This paper presents a plan and guidelines that were drawn for Korean based research carried out on the fire-resistance of CFT columns. This research was carried out by reviewing the Korean regulations related to the fire-resistance of CFT columns and examining studies which had been made in Korea as well as overseas. The first phase of the study plan was to compare the fire-resistance of square CFT columns without fire protection (obtained through fire-resistance tests and numerical analyses) with estimated values (obtained through fire-resistance design formulas proposed in Korea and overseas). This comparison provided conclusions as outlined below. Fire-resistance tests conducted in this study proved that, when the actual design load is taken into consideration, square CFT columns without fire protection are able to resist a fire for more than one hour. A comparison was made of test and analysis results with the fire-resistance time based on the AIJ code, the AISC design formula and the estimation formula suggested for Korea. The results of this comparison showed that the test and analysis results for specimens SAH1, SAH2-1, SAH2-2 and SAH3 were almost identical with the AIJ code, the AISC design formula and estimation formula. For specimens SAH4 and SAH5, the estimation formula was more conservative than the AIJ code and the AISC design formula. It was necessary to identify the factors that have an influence on the fire-resistance of CFT columns without fire protection and to draw fire-resistance design formulas for these columns. To achieve this, it is proposed that numerical analyses and tests be conducted in order to evaluate the fire-resistance of circular CFT columns, the influence of eccentricity existing as an additional factor and the influence of the slenderness ratio of the columns. It is also suggested that the overall behavior of CFT structures without fire protection within a fire be evaluated through analysis simulation.

Keywords: fire resistance; concrete-filled steel square tube column; without fire protection; constant central axial load; numerical analysis; fire-resistance test.

1. Introduction

Due to the heat storage effect of the concrete filled interior, concrete-filled steel tube (CFT) columns are able to resist a fire even when they are not covered with fireproofing materials, as shown in Fig. 1.

*Corresponding Author, E-mail: smc@uos.ac.kr

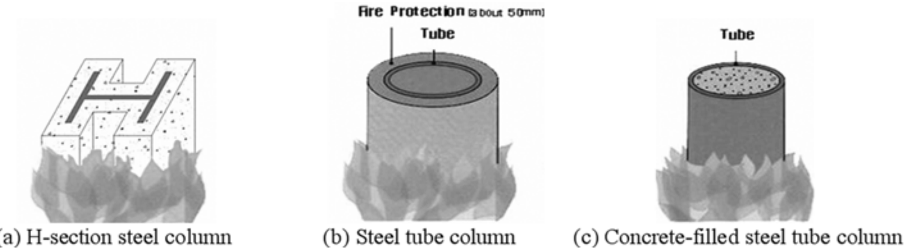

Fig. 1 Fire Resistance of CFT column

Fire-resistance studies conducted in Europe and North America focused on CFT columns (Lie *et al*. 1992, Newman *et al*. 2001, Al-Khaleefi *et al*. 2002, Renaud *et al*. 2003, Zha 2003). In Europe, such studies were a part of the research on composite construction, and date back to the 1970s and 1980s. The purpose of these studies was to develop CFT columns so they would be able to resist a fire for more than a specified period of exposure to fire without fire protection. Such studies resulted in the fire-resistance design of CFT columns without fire protection (Kodur *et al*. 1995, 1999, Bergmann *et al*. 1995, Wang 2000, 2002, Tan *et al*. 2004, Renaud *et al*. 2006, Ding *et al*. 2008). These studies subsequently evolved into research on how to improve the fire-resistance of the concrete inside the columns, in order to expand the application of CFT columns for high-rise buildings (Yin *et al*. 2006, Kodur 2005, 2007). Studies have also been conducted on the application of reinforced high strength concrete and steel fiber reinforced high strength concrete (Kodur *et al*. 1996, 1997, 1998, 2005, Saito *et al* 2001). Studies in Japan and China have focused on how to reduce the thickness of the protection by improving the fire-resistance of the CFT columns (Sakumoto *et al*. 1994, Han 2001, Han *et al*. 2003a, 2003b). As shown in Fig. 3, up to the 1990s, most of the studies that were conducted in Korea and overseas that were concerned with how to improve the fire-resistance of CFT columns suggested the use of CFT columns with steel or steel fiber reinforcement of the concrete inside the columns. While many studies since 2000 concerning the application of a fireproofing material on the column surface have been conducted in Japan and China, studies conducted in Europe and the U.S. have focused on high strength concrete or FRP-reinforced CFT columns.

In Korea, through experimental and analytical studies (Choi *et al*. 1998, 2000, 2003, 2005, 2006, 2007) on the fire-resistance of CFT columns, the fire-resistance of CFT columns were verified from the late 1990s to the early 2000s. However, CFT columns without fire protection were not used in actual construction due to the specification-based design (Fig. 2) as prescribed in municipal laws. Recently, it became highly feasible to develop and readjust fire-resistance design to a realistic level when a clause that stated, 'what is of fire-resistant structure based on the performance design approved by the President of KICT (Korea Institute of Construction Technology) was introduced in June 2006 to the municipal laws in the clauses that constitute what is acceptable in terms of fire-resistance approval.

In February 2007, square CFT columns without fire protection were used in the actual construction of the parking garage of Samsung Electronics, as shown in Table 1 and Fig. 4 (Han *et al*. 2007). This was the first time this type of construction was used in Korea, and it was the first case in Korea where the fire-resistance of CFT columns was authorized through [individual certification]. However, in order to realize the performance based fire-resistance design for CFT columns, more tests and analytical studies on the fire-resistance of these structures needed to be made. In order to prove the fire-resistance of a CFT structure and to apply it in actual construction, influential factors and improved fire-resistance design formulas should be suggested through various tests and analyses of CFT structures.

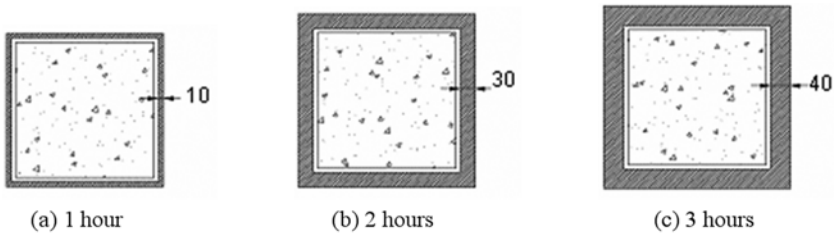

Fig. 2 Thickness of fireproof covering of CFT columns in Korea (mm)

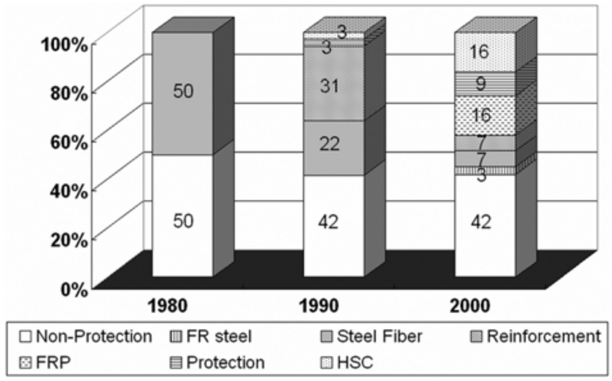

Fig. 3 Breakdown of the studies on CFT columns

Table 1 Construction overview of the structure with square CFT columns without fire protection

Usage of building	Construction period	Scale		Structure
		Area (m^2)	No. of floors	
Parking garage	2006.8-2007.2	65,000	2 below and 2 above ground	R.C(underground) + CFT(above ground)

Fig. 4 Square CFT columns without fire protection applied to the parking garage of Samsung Electronics

Accordingly, the purpose of this study was to review the fire-resistance of CFT column through a fire-resistance test and numerical analysis of square CFT columns without fire protection under constant axial load. A comparison was also made between the estimated values obtained from existing design formulas proposed abroad and the estimation formula proposed in Korea in order to prove the fire-resistance of square CFT columns without fire protection.

2. Fire-resistance analysis of CFT columns without fire protection based fire-resistance tests

2.1 Specimens and test method

Taking into consideration the application of CFT columns in actual construction, as shown in Fig. 4, 9mm thick column specimens of 300 mm and 350 mm in diameter were made. The effective heating length of the specimens was 2,400 mm, 2,800 mm and 3,000 mm. A 20 mm thick endplate was welded to both ends of each specimen. Two 20 mm diameter holes were made at 510 mm, 1,430 mm and 2,350 mm points from the top endplate of each specimen in order for vapor to be released (Fig. 5). SPSR 400 steel was used and Table 2 shows the mechanical properties of the steel produced in accordance with KS B 0801. Concrete with design strength of 23.5 MPa and 35.3 MPa was used. Table 3 shows the results of the compression test conducted in accordance with KS F 2405. For this test, the concrete was 30-60 days old and the moisture content was approximately 6.6%. A top press-in method was used for concrete filling. After filling, the top end of each column was sealed with plastic in order to cure the concreted surface. Columns were not covered with fireproofing materials.

12 square CFT column specimens without fire protection (Table 4) were produced for a full-scale experiment to evaluate fire-resistance. As shown in Fig. 6, an axial load was applied to the specimens from both the top and the bottom of the heating furnace. The axial load ratio was set with the field application taken into consideration (Fig. 4) and a 3,000 kN compressor was used. A constant axial load was applied to the center of the columns, 15 minutes before heating. Heating was applied during the application of the load, in accordance with the standard fire curve (KS F 2257-1, 2005), as shown in Fig. 7. This was almost identical to the ISO-834 standard fire temperature curve (ISO 834, 1999).

Elongation caused by thermal expansion and shrinkage was measured by the LVDT mounted to a hydraulic cylinder. The test was concluded when the amount of axial shrinkage exceeded 1/100 of the effective heating length or when deformation reached 3L/1000 mm/min, since such cases assumed that the load capacity of square CFT column without fire protection was lost.

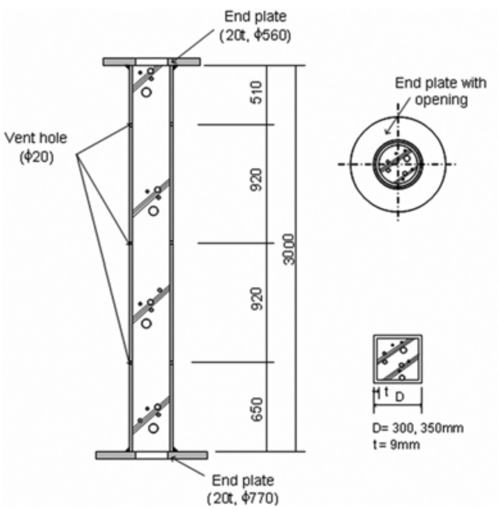

Fig. 5 Specimen details and points of temperature measurement

Table 2 Mechanical properties of steel

Thickness(mm)	Steel grade	Yield stress(MPa)	Tensile strength(MPa)	Elongation(%)
9	SPSR 400	363	490	33

Table 3 Mechanical properties of concrete

Age (days)	Compressive strength (MPa)	1/3 Fc secant modulus (GPa)
28	27.5	24.5
28	37.8	28.4

Table 4 Test variables

Specimen	Cross-sectional size (mm)	fck (MPa)	Na/Nc (Axial load ratio)	Na (Axial load)(kN)	Le (Effective heating length) (mm)	t (Fire resistance time) (min.)	
						Test	Analysis
SAH1	□– 300 × 9	37.8	0.58	1,570	3,000	57	54
SAH2-1	□– 300 × 9	37.8	0.50	1,410	2,400	44	63
SAH2-2	□– 300 × 9	37.8	0.51	1,390	3,000	53	63
SAH3	□– 300 × 9	37.8	0.45	1,225	3,000	90	80
SAH4	□– 300 × 9	37.8	0.38	1,025	3,000	171	109
SAH5	□– 300 × 9	37.8	0.32	884	3,000	180*	121
SAL3	□– 300 × 9	27.5	0.45	843	3,000	80*	108
SAL4	□– 300 × 9	27.5	0.40	745	2,400	130*	124
SBH2	□– 300 × 9	37.8	0.50	840	2,800	108	92
SBH4	□– 300 × 9	37.8	0.40	1,560	3,000	140*	128
SBL2	□– 300 × 9	27.5	0.50	1,295	3,000	80*	114
SBL4	□– 300 × 9	27.5	0.40	1,040	2,800	160*	149

Shape of cross-sectional area	Size of cross-sectional area		f_{ck}		N_a/N_c (Axial load ratio (-1, 2 : number))				
S	A	B	H	L	1	2	3	4	5
Square	300	350	37.8	27.5	0.58	0.5 / 0.51	0.45	0.38 / 0.4	0.32

* is time that heating is finished but the specimen was not failed.

The concrete temperate was measured at 5 points (Fig. 5): at the center of the cross-sectional area; at a 1/4 point of the cross-sectional area; on the surface; at a diagonally 1/4 point; and on the diagonal surface. The temperature of the steel tube was measured at 6 points: both sides at 900 mm each, and at points at 1,500 mm and 2,100 mm from the bottom end of the column.

2.2 Test results

2.2.1 Temperature distribution

The temperature distribution inside the cross-sectional area of CFT columns without fire protection during heating was compared with the standard heating curve, as shown in Fig. 8. Since the steel temperature rose at a slower rate than the standard heating curve, the former was lower than the latter until the 60 minutes point. Subsequently, the steel temperature almost approached the standard heating curve.

Fig. 14 shows the concrete temperature measured at the concrete surface, at a point at a 1/4 of the cross-sectional area and at the center of the cross-sectional area of each specimen. At the concrete surface,

Fig. 6 Heating furnace

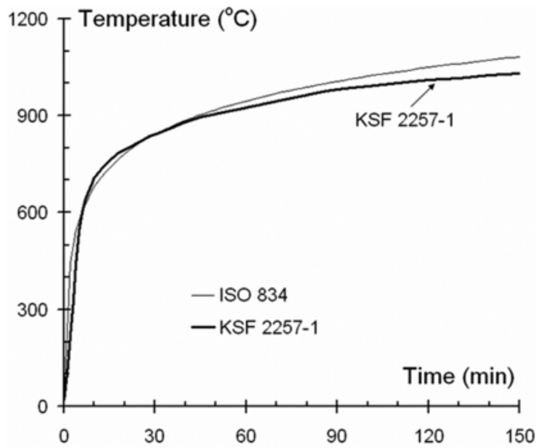

Fig. 7 Standard heating curves (KSF 2257-1, 2005)

the temperature rose at a slower rate than the standard heating curve at the early stage of heating, but it was almost identical to the standard heating curve from the 100 minutes point. At the center of the concrete, the temperature rose very slowly due to the insulation of the concrete. The temperature measured at 120 minutes was as low as 200°C. Such results show that CFT columns without fire protection are fire-resistant and can be used as fire-resisting material. The temperature of specimens SAH1 and SAH4 dropped rapidly from 300°C to 100°C, at the 20 minutes point, from 300°C to 100°C, then remained constant for approximately 20 minutes and subsequently rose suddenly to over 400°C. This result implies that if the axial load is strong, then the heated vapor inside the CFT column is instantly discharged through the holes, causing a temperature drop and a subsequent rise as it was reheated.

2.2.2 Fire-resistance

As shown in Fig. 9, specimen SAH5 presented a maximum axial tensile deformation of 5.3 mm at the

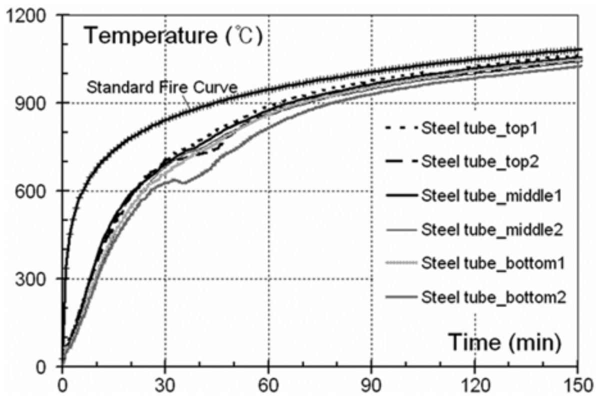

Fig. 8 Temperature distribution on steel tube surface

24 minutes point. It also presented a maximum axial compressive deformation of 7.2 mm at the 180 minutes point (the point of test closure), which was approximately 25% of the maximum permissible compressive deformation of 30 mm. This implies that specimen SAH5 has a much higher fire-resisting performance. Specimen SAH4 reached a maximum axial tensile deformation of 14.8 mm at 17 minutes and presented a rapid increase of compressive deformation from 14.7 mm to 73.7 mm at 172 minutes. This signifies that the load capacity of the column had been lost. SAH1 presented a maximum axial tensile deformation of 17mm at 16 and 18 minutes and a rapid rise of compressive deformation from 7 mm to 31.5 mm at 58 minutes. This implies that the load capacity of the column had been lost. An axial load ratio of 0.51 or 1,390 kN was applied to SAH2-2, which could not resist fire for more than 60 minutes, while the SAH3 specimen to which an axial load ratio of 0.45 (1,225 kN) was applied, demonstrated a fire-resistance of 90 minutes. SAH3 is the specimen of the CFT column without fire protection that was applied to the parking garage of Samsung Electronics (Figure 4 and Table 1). This result therefore demonstrates that CFT columns without fire protection that have the actual design load taken into consideration can resist fire for more than 1 hour. In developed countries such as Europe and Japan, it has already been proven that CFT columns without fire protection provide fire-resistance for more than 1 hour and studies on how to improve fire-resistance have been actively conducted.

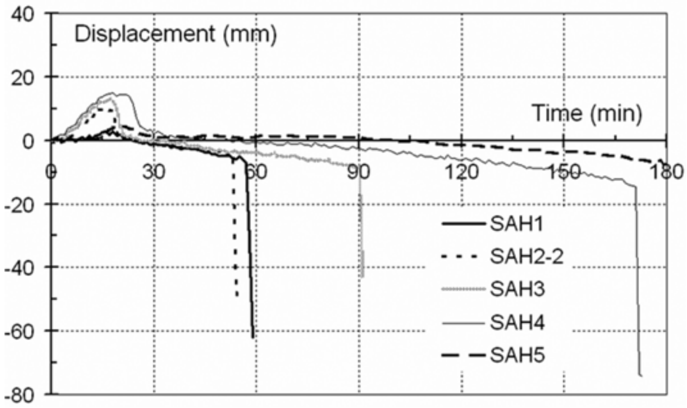

Fig. 9 Axial deformation caused by the axial load ratio of CFT column

2.2.3 Failure pattern

As shown in Fig. 10, subsequent to the fire-resistance test, local buckling was observed at a point 1/3 from the top end of the CFT column and flexural deformation was presented from the central axis.SAH4 and SAH5 specimens, which resisted fire for more than 2 hours, showed a separation of the steel surface (Fig. 10) but did not present local buckling.

3. Fire-resistance analysis of CFT columns based on numerical approaches

3.1 Numerical approaches

3.1.1 Objects

For the comparison between numerical analysis results and test results, a numerical analysis was conducted of 300mm and 350mm diameter CFT columns. Analysis variables were selected that were identical to the test variables in Table 4. The values obtained from the material test shown in Tables 2 and 3 were applied as the steel strength and concrete strength in order to provide conditions that were identical to the actual columns. The cross-sectional area of columns was divided, as shown in Fig. 11, in order to calculate the temperature, deformation and stress of the CFT columns.

3.1.2 Thermal properties of materials

In Korea, thermal properties formulas for structural materials at high temperatures have not been established. The thermal properties of concrete inside the CFT columns at a high temperature are influenced by the moisture content of the concrete, the type of aggregate, the mix proportion, the temperature and the air content. The material model of the EUROCODE (Eurocode 4; 2003) (Figs. 12, 13) was employed in order to obtain the thermal characteristics of the steel tube and concrete of the CFT column.

3.1.3 Method of numerical analysis

A heat transfer analysis was carried out for the CFT columns, with the thermal properties of the

(a) Local buckling at column

(b) Surface separation after heating

Fig. 10 Status of CFT columns after fire-resistance test

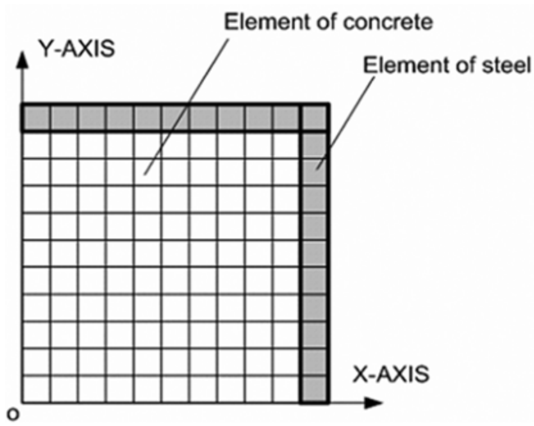

Fig. 11 Analysis model (1/4 cross-sectional division)

column materials taken into consideration. This was conducted in order to measure the temperature distribution inside the cross-sectional area of the columns. The standard heating curve (KSF 2257-1, 2005) in Fig. 7 was applied in order to realize a fire.

For a 2-dimensional temperature prediction, Eq. (1), representing the relationship between temperature

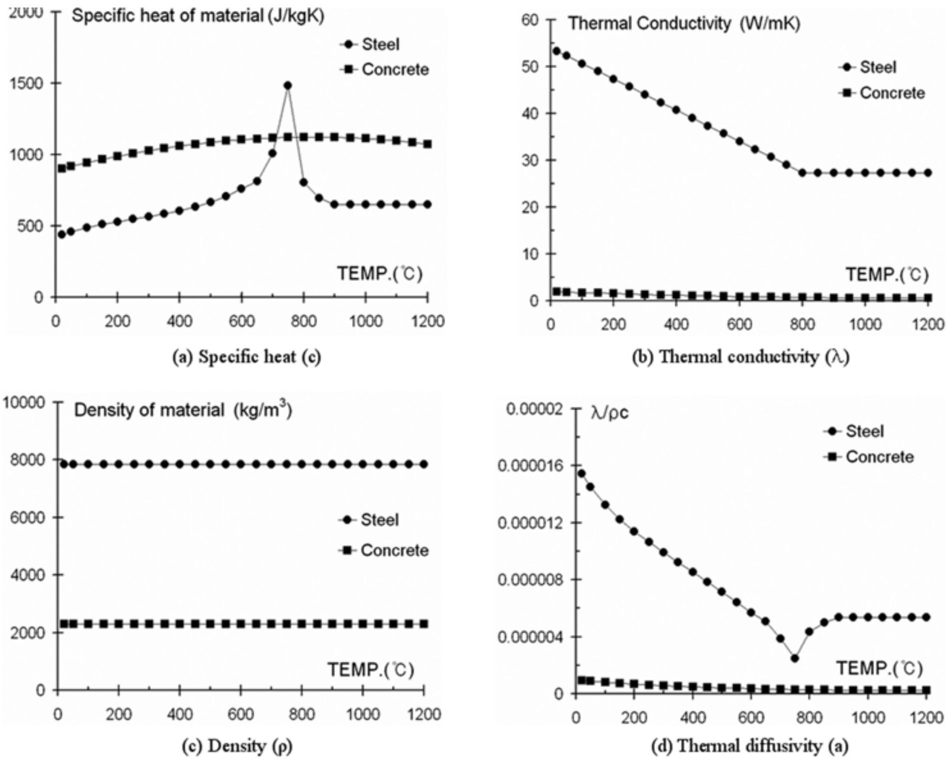

Fig. 12 Thermal properties of materials (steel, concrete)

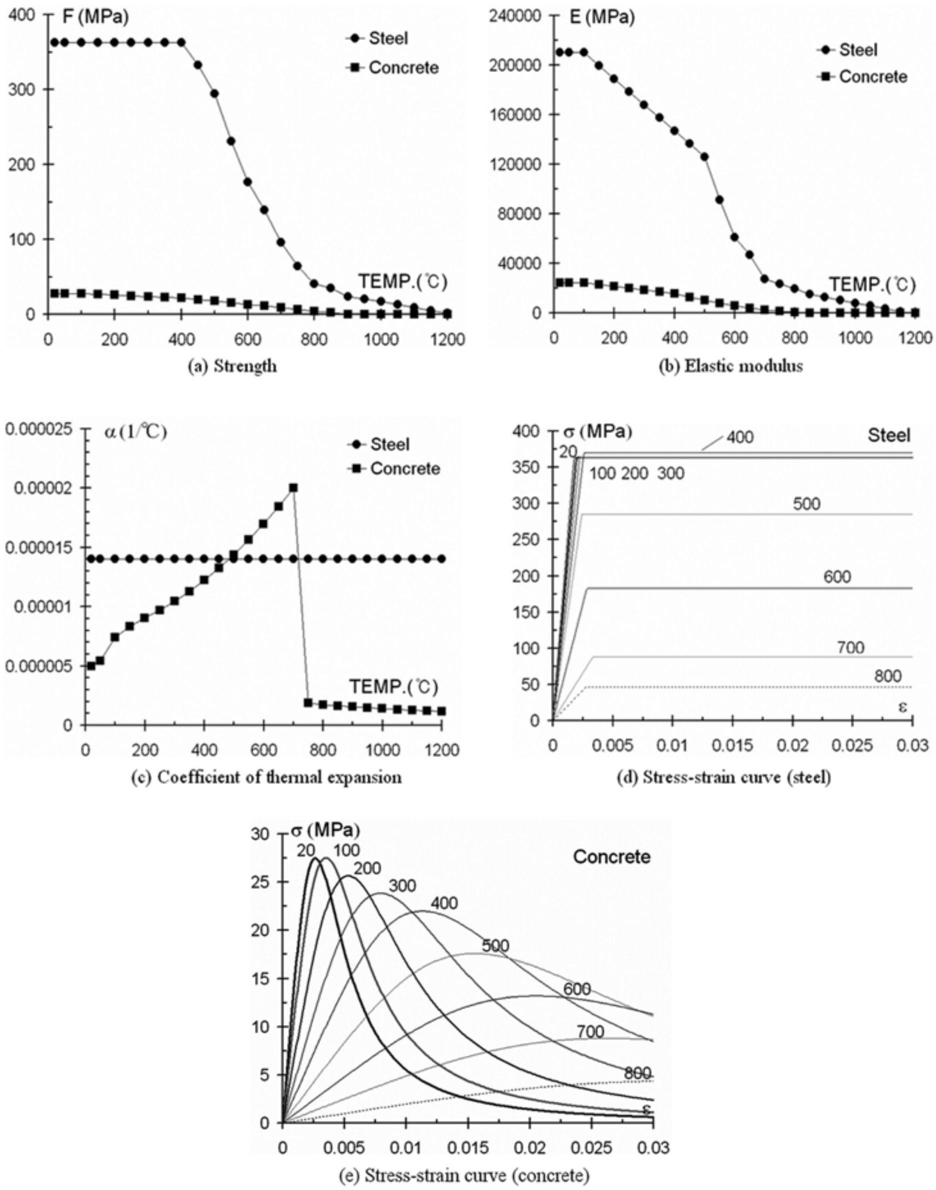

Fig. 13 Mechanical properties of materials (steel, concrete)

changes in minor elements and the amount of heat inflow, was given as follows:

$$\frac{\partial T}{\partial t} = a\left(\frac{\partial^2 T}{\partial x^2} + \frac{\partial^2 T}{\partial y^2}\right) + \frac{Q}{c \cdot \rho}, \quad \left(a = \frac{\lambda}{c \cdot \rho}\right) \tag{1}$$

where, a is the thermal diffusivity, c is the specific heat, ρ is the density, λ and is the thermal conductivity (Fig. 12).

Based on this formula, the finite difference method was applied by the Crank-Nicolson Method in order to derive Eq. (2) for the temperature inside the cross-sectional area from Eq. (1).

$$\frac{T_{i,j}^{k+1} - T_{i,j}^{k}}{\Delta t} = \frac{a}{2}\left(\frac{T_{i+1,j}^{k+1} - 2T_{i,j}^{k+1} + T_{i-1,j}^{k+1}}{\Delta x^2} + \frac{T_{i,j+1}^{k+1} - 2T_{i,j}^{k+1} + T_{i,j-1}^{k+1}}{\Delta y^2}\right.$$
$$\left. + \frac{T_{i+1,j}^{k} - 2T_{i,j}^{k} + T_{i-1,j}^{k}}{\Delta x^2} + \frac{T_{i,j+1}^{k} - 2T_{i,j}^{k} + T_{i,j-1}^{k}}{\Delta y^2}\right) + \frac{Q}{c \cdot \rho} \tag{2}$$

Eq. (3) was evolved from Eq. (2) in order to predict the temperature change in each element. The amount of heat inflow constituting of a boundary condition was given as Eq. (4). With thermal convection and radiation taken into consideration, the heat flow rate was calculated as Eq. (5).

$$T_{i,j}^{k+1} = \frac{1}{2(1 + c_x + c_y)}[c_x(T_{i+1,j}^{k+1} + T_{i-1,j}^{k+1} + T_{i+1,j}^{k} + T_{i-1,j}^{k})$$
$$+ c_y(T_{i,j+1}^{k+1} + T_{i,j-1}^{k+1} + T_{i,j+1}^{k} + T_{i,j-1}^{k}) + 2(1 - c_x - c_y)T_{i,j}^{k} + 2c_q Q] \tag{3}$$

Here, $c_x = \frac{a \cdot \Delta t}{\Delta x^2}$, $c_y = \frac{a \cdot \Delta t}{\Delta y^2}$, $c_q = \frac{\Delta t}{c\rho}$

$$Q = l \times q(T_s, T_f) \tag{4}$$

where, l = length between i and j
Q = rate of heat flow per unit area
T_s = average surface temperature
T_f = temperature of heating furnace

$$q = A(T_f - T_s) + V\sigma\varepsilon(\theta_f^4 - \theta_f^4) \tag{5-a}$$

$$\varepsilon = \frac{1}{\frac{1}{\varepsilon_f} + \frac{1}{\varepsilon_s} - 1} \tag{5-b}$$

here, A = thermal convection coefficient (23W/m^{2}K)
V = Radiation angle coefficient (1.0)
σ_{SB} = Stefan-Boltzman constant (5.67 × 10^{-8}W/m^{2}K^4)
ε_s = Steel tube thermal radiation (0.8)
θ_f = Furnace absolute temperature
θ_s = Steel tube surface absolute temperature

With the temperature distribution data and mechanical properties of materials taken into consideration, a thermal stress analysis was conducted in order to evaluate the behavior and fire-resistance of CFT columns in a fire. Based on the temperature distribution inside the cross-sectional area obtained from the temperature analysis, 2 numerical analyses were made for the fire-resistance of CFT columns under central axial load.

■ Maximum load capacity

Multiplying the cross-sectional area of each element (steel, concrete) by its ultimate strength against temperature (Fig. 13 (a)) produced Eq. (6) for load capacity as follows:

$$N = \sum_{i,j}^{n} F(i,j) \cdot dA(i,j) \tag{6}$$

where, F(i,j) is the ultimate strength of the element; dA(i,j) is the cross-sectional area of the element.

■ Axial deformation behavior

In a fire, axial deformation of steel and concrete is produced by the increased deformation caused by thermal expansion and axial load (Eq. (5-a)). Stress is decided by the stress-strain relationship of steel & concrete against temperature changes (Fig. 13-(d)). Once the equilibrium with external force (central axial load) is achieved following a process of trial and error, stress is finally calculated (Eq. (5-b))

$$\varepsilon = \varepsilon_{th}(T) + \varepsilon_{\sigma}(\sigma, T) \tag{7}$$

where, ε = total strain, σ = corresponding stress, T = temperature, ε_{th} = thermal expansion strain due to increasing temperature without any load applied, ε_{σ} = instantaneous stress-related strain that is a function of the stress and temperature.

3.2 Verification of the fire-resistance of CFT columns based on numerical analysis

3.2.1 Verification of temperature distribution inside the cross-sectional area

A comparison was made with the results of the fire-resistance test conducted in Chapter 2 in order to analyze and verify the reliability of the prediction of temperature distribution inside the CFT column cross-sectional area that was obtained through numerical analysis. As shown in Fig. 14, numerical analysis results were either almost identical with, or were more conservative than, the test results. This implies the prediction of a higher temperature during the same time length of fire-resistance.

3.2.2 Verification of stress analysis

As shown in Fig. 15, the changes were analyzed of the maximum load capacity ratio (N/N_c) of the CFT columns. For some specimens, the test was concluded before failure was reached. The arrows in Fig. 15 indicate such cases. For the SAH2 specimen, the maximum load capacity that was obtained from numerical analysis was slightly higher than that obtained from the test. For all other specimens, the maximum load capacity obtained from numerical analysis was either almost identical with, or was more conservative than, the test value.

Axial deformation behavior caused by the deterioration of load capacity during a fire was compared

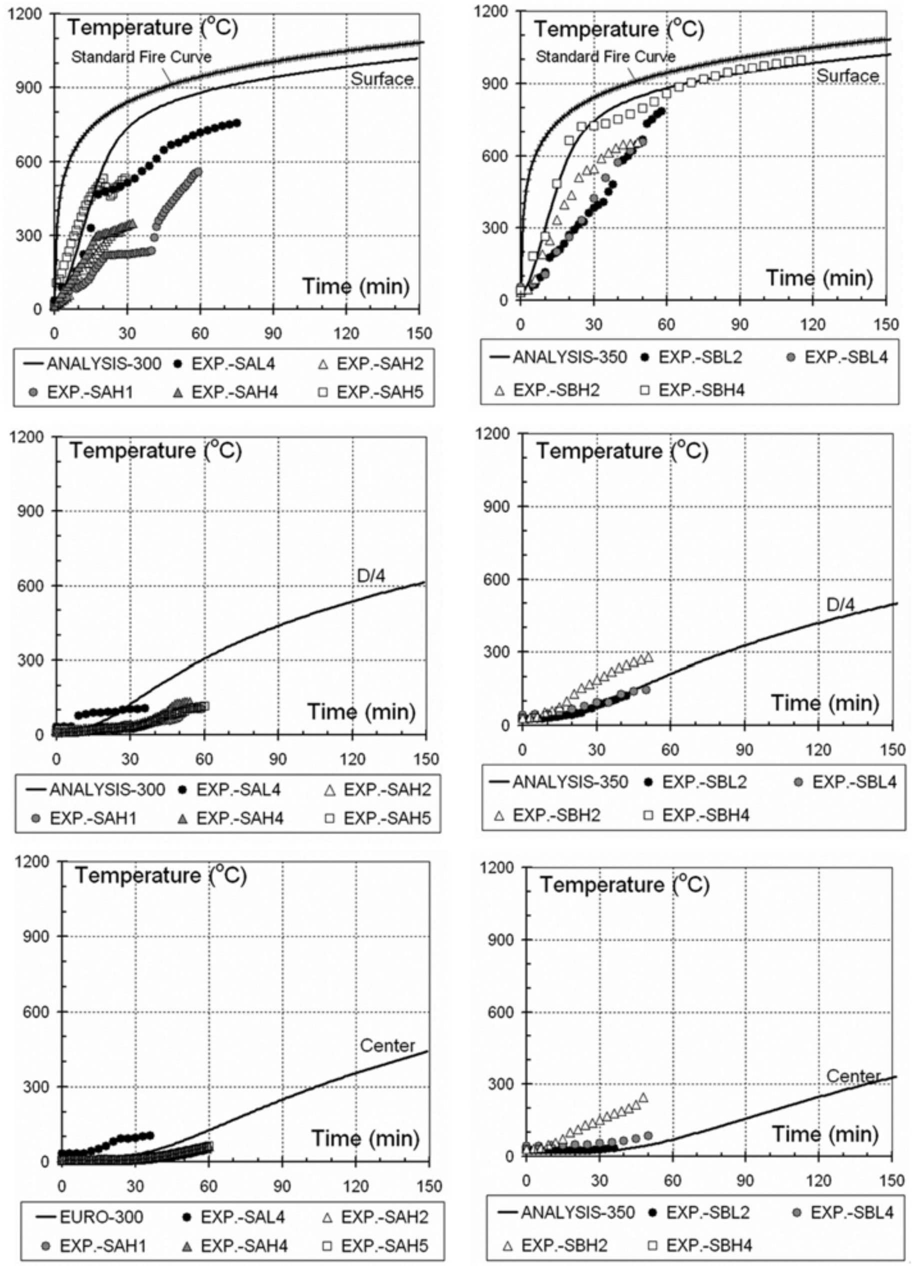

(a) □-300 × 300 × 9 (b) □-350 × 350 × 9

Fig. 14 Comparison of temperature distribution between analysis values and test results

with test values as shown in Fig. 16. For the SAH2 specimen, the fire-resistance associated with maximum load capacity ratio was higher than the test value, as shown in Fig. 15. For SAH2, the axial deformation behavior, caused by a temperature rise, was similar to that observed during the test, until failure was reached. For specimens SAH1, SAH2 and SAH3, the thermal expansion deformation at the

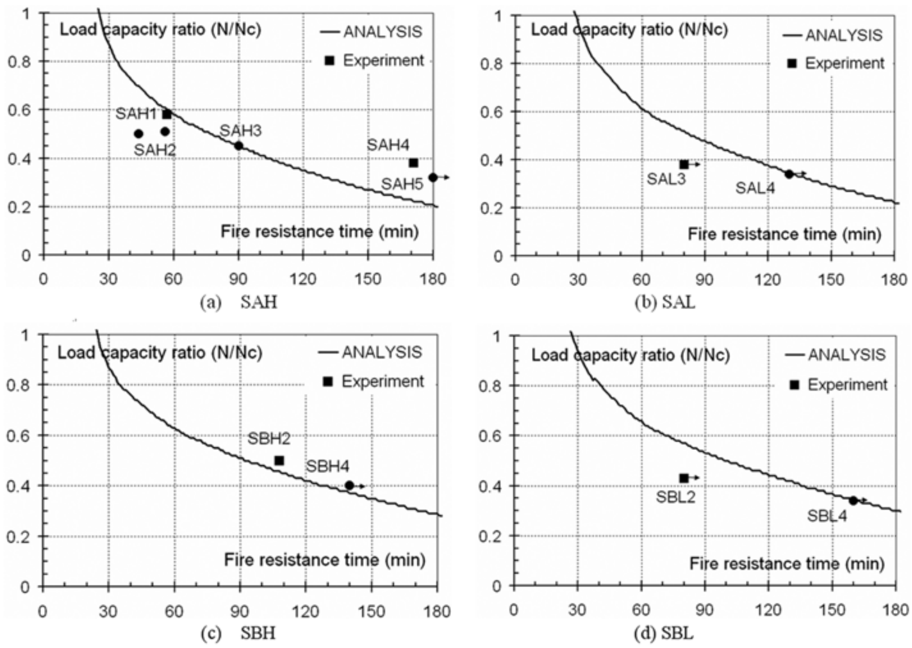

Fig. 15 Comparison of fire resistance between analysis and test - (1)

steel tube was observed and the shrinkage deformation of the concrete followed. Due to a high axial load, these specimens subsequently suddenly failed without presenting enough axial deformation.

A high axial load accompanied the expansion of the steel tube, followed by marginal shrinkage deformation and then failure. When the axial load was weak, the shrinkage deformation was very slow and most of the test values were higher than the analysis values in terms of fire-resistance.

A comparison between axial deformation behavior based on numerical analysis and that in the test results demonstrated that the analysis values were either identical with, or were slightly more conservative than, the test values.

3.3 Comparative analysis of fire-resistance with various design codes

As shown in Fig. 17, test and analysis results were compared with the fire-resistance time obtained from AIJ Code (Eq. 10) (ANUH 1997), AISC design formula (Eq. 9) (Ryddy *et al*. 2003) and formula (Eq. 8) suggested in Korea (Choi *et al*. 2000). In accordance with the AISC provision that limits fire-resistance time to 2 hours, specimens SAH4 and SAH 5 were excluded since they both had a fire-resistance time in excess of 2 hours.

As demonstrated in Fig. 17, the test and analysis results for specimens SAH1, SAH2-1, SAH2-2 and SAH3 were almost identical with the AIJ code, the AISC design formula and estimation formula suggested in Korea. For specimens SAH4 and SAH5, the estimation formula was more conservative than the AIJ code and the AISC design formula.

■ Estimation formula suggested in Korea (Choi *et al*. 2000):

$$t = (1 / \beta)\ ln((N_a \times 10^3) / (f_{ck} \times A_c)) \tag{8}$$

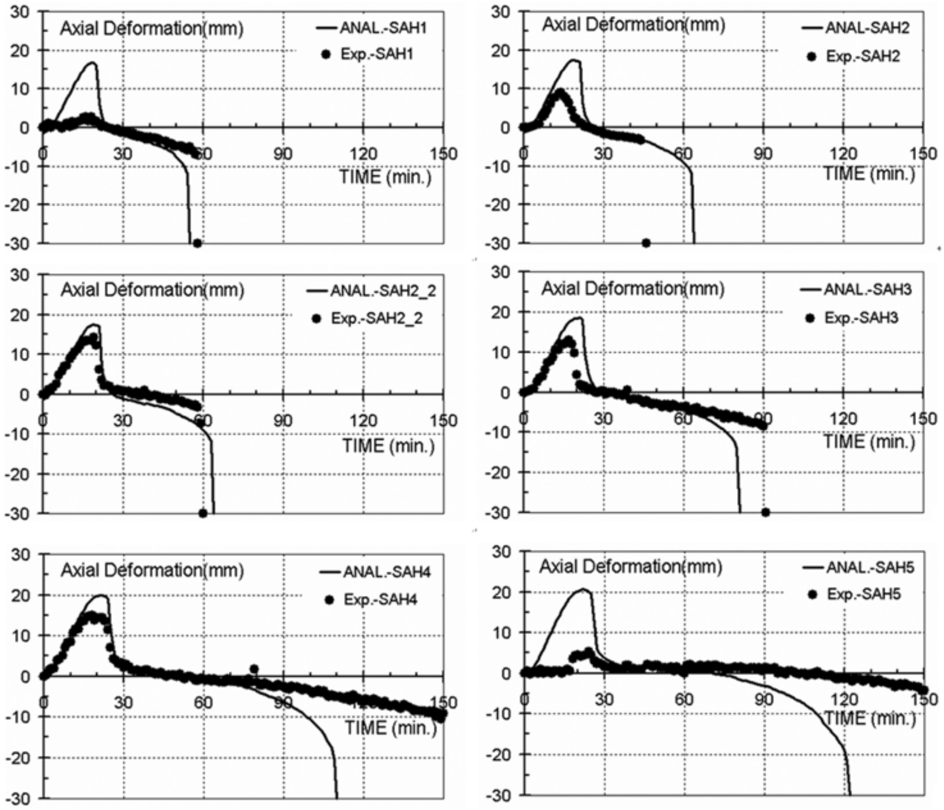

(a) SAH

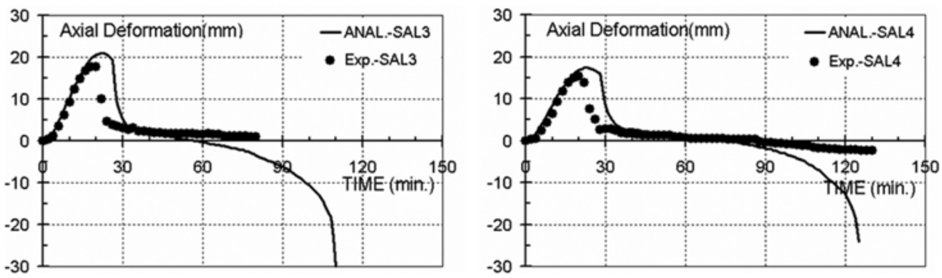

(b) SAL

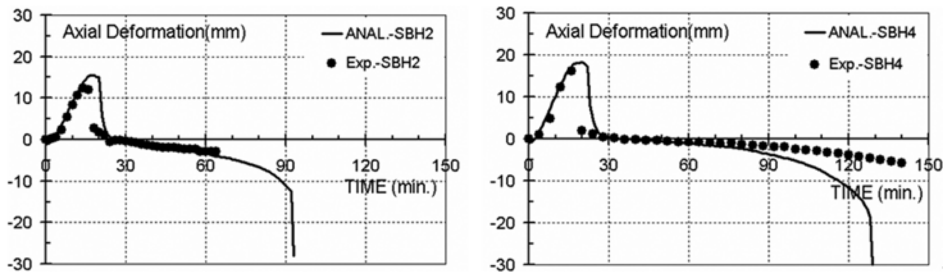

(c) SBH

Fig. 16 Comparison of axial deformation between analysis and test - (2) Continued...

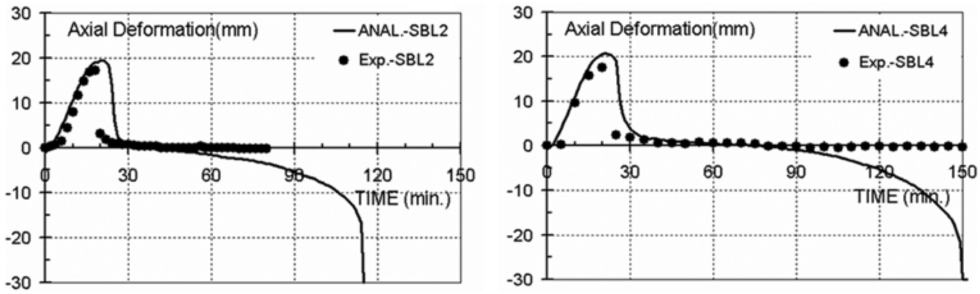

(d) SBL

Fig. 16 Comparison of axial deformation between analysis and test - (2)

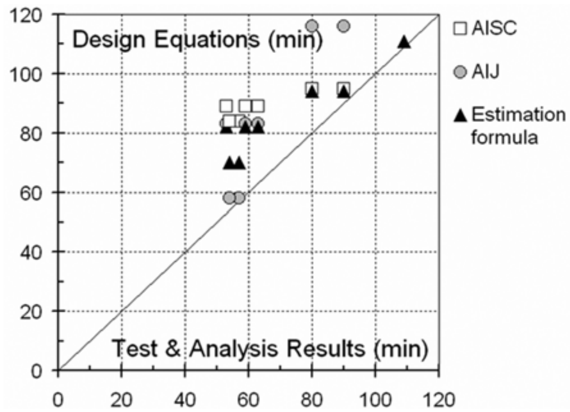

Fig. 17 Comparison of fire-resistance between test & analysis results and various design formulas

where, t = fire resistance time (min.) (for only square CFT columns)
D_c = width of in-filled concrete (mm)
N_a = applied axial load (kN)
f_{ck} = specified 28 day concrete strength (MPa)
A_c = cross-sectional area (mm^2)
N_c ($= f_{ck} \times A_c$) = compressive resistance of concrete core (kN)
β = factor of fire resistance time

■ AISC (Ryddy *et al*. 2003)

$$t = f_1 \cdot \left(\frac{f_{ck}+20}{L_e - 1000}\right) \cdot D_c^2 \cdot \sqrt{\frac{D_c}{N_a}} \tag{9}$$

where, t : fire resistance time (min.)($\leq$ 120 min.)
f_{ck} : specified 28 day concrete strength (MPa)
N_a : applied axial load (kN)
D_c : width of in-filled concrete (mm)
L_e : Effective heating length (mm) (2,000 ~ 4,500 mm)

f_1 : 0.06(Siliceous), 0.07(Carbonate)

- Fire-resistance design formula in Japan (ANUH 1997)

$$N_a = 21.77 \cdot A_c \cdot f_{ck} \cdot \left(\frac{1}{t}\right)^{0.367} \tag{10}$$

where, A_c : cross-sectional area of concrete (mm^2)
f_{ck} : specified 28 day concrete strength (MPa) (23.5MPa $\leq f_{ck} \leq$ 41.2MPa)
N_a : applied axial load (kN)
t : fire resistance time (min.)

4. Conclusions

This research was carried out in Korea and reviewed the regulations related to the fire-resistance of CFT columns and examined studies conducted in Korea and overseas. The first phase of the plan was to compare the fire-resistance of square CFT columns without fire protection that were obtained through fire-resistance tests and numerical analysis, with the estimated values that were obtained through fire-resistance design formulas proposed in Korea and overseas. The results of this comparison provided the following conclusions:

Fire-resistance tests conducted in this study proved that square CFT columns without fire protection that take into consideration the actual design load are able to resist fire for more than one hour. Among the specimens in this study, the □-300 × 300 × 9 CFT column demonstrated a fire-resistance time of ninety minutes in a load heating test under an axial load ratio of (N/Nc) 0.45(1250kN) and it acquired individual certification for over 1 hour fire-resistance (Fig. 4, Table 1).

Local buckling was observed at a point 1/3 from the top end of the column and flexural deformation occurred from the central axis.

With regard to axial deformation behavior and maximum load capacity during a fire, it was confirmed that analysis values were either almost identical with, or were slightly more conservative than, the test values. Consequently, it is reasonable to conclude that the prediction of the fire-resistance of CFT columns based on numerical analysis is reliable. With regard to fire-resistance time, test and analysis results were compared with those from the AIJ Code, the AISC design formula and the estimation formula suggested in Korea. Test and analysis results for specimens SAH1, SAH2-1, SAH2-2 and SAH3 were almost identical with the AIJ code, the AISC design formula and estimation formula suggested in Korea. For specimens SAH4 and SAH5, the estimation formula was more conservative than the AIJ code and the AISC design formula.

The factors that influence the fire-resistance of CFT columns without fire protection needed to be identified. Fire-resistance design formulas also needed to be drawn for these columns by conducting the study on the fire-resistance of CFT columns without protection. To achieve this, it is proposed that numerical analyses and tests be conducted in order to evaluate the fire-resistance of circular CFT columns, the influence of eccentricity existing as an additional factor and the influence of the slenderness ratio of the columns. It is also suggested that the overall behavior of CFT structures without fire protection in a fire be evaluated through analysis simulation in order to provide fire-resistance design formula for CFT columns without fire protection and to develop fire-resistance design technologies.

5. Acknowledgments

This study was conducted with the support of the Construction Technology Innovation Program of the R&D Project (Grant 06 Construction Consequence D07) funded by the Ministry of Construction & Transportation of Korean government and the National Research Laboratory (Grant R0A-2007-000-10047-0). This financial support is greatly appreciated.

Notation

A	:	thermal convection coefficient ($23\text{W/m}^2\text{K}$)
A_c	:	cross-sectional area of concrete (mm^2)
a	:	thermal diffusivity ($\text{Wm}^2\text{/J}$)
c	:	specific heat (J/kgK)
$dA(i,j)$	:	the cross-sectional area of the element
D_c	:	the width of in-filled concrete (mm)
$F(i,j)$	:	the ultimate strength of the element
f_{ck}	:	specified 28 day concrete strength (MPa)
f_1	:	material parameter (0.06 (siliceous), 0.07 (carbonate))
L_e	:	effective heating length (mm)
l	:	length between i and j
Na	:	applied axial load (kN)
N_c	:	the compressive resistance of concrete core (= $f_{ck} \times A_c$) (kN)
N	:	maximum load capacity (kN)
Na/N_c	:	axial load ratio
N/N_c	:	maximum load capacity ratio
Q	:	the rate of heat flow per unit area
T	:	corresponding temperature
t	:	fire resistance time (min.)
T_f	:	the temperature of heating furnace
T_s	:	average surface temperature
V	:	radiation angle coefficient (1.0)
σ	:	corresponding stress
σ_{SB}	:	Stefan-Boltzman constant ($5.67 \times 10^{-8}\text{W/m}^2\text{K}^4$)
ε	:	total strain
σ_s	:	steel tube thermal radiation (0.8)
σ_{th}	:	thermal expansion strain due to increasing temperature without any load applied
ε_σ	:	instantaneous stress-related strain that is a function of the stress and temperature
α	:	coefficient of thermal expansion
β	:	factor of fire resistance time
λ	:	thermal conductivity (W/mK)

ρ : density (kg/m^3)
θ_f : furnace absolute temperature
θ_s : steel tube surface absolute temperature

References

Association of New Urban Housing (ANUH) (1997), Design Guide Manual for Concrete-filled Steel Tube Columns, Japan.

Abdullateef M. Al-Khaleefi, Mohammad J. Terro, Alex P. Alex and Yong Wang (2002), Prediction of Fire Resistance of Concrete Filled Tubular Steel Columns using Neural Networks, *Fire Safety J.*, **37**, Issue 4, 339-352.

C. Renaud, J.M. Aribert and B. Zhao (2003), Advanced Numerical Model for the Fire Behaviour of Composite Columns with Hollow Steel Section, *Steel Compos. Struct.*, **3**(2), 75-95.

C. Renaud, J.M. Aribert and B. Zhao, Effect of differential thermal stresses on the fire resistance of composite columns with hollow section, *ASCE Conference Proceedings of the Composite Construction in Steel and Concrete V*, 607-618, July 18-23, 2006, Mpumalanga, South Africa.

European Committee for Standardization (2003), Eurocode No. 4: Design of Composite Steel and Concrete Structures, Part 1.2: Structural Fire Design, DD ENV 1994-1-2, British Standards Institution, UK.

G.M. Newman and W.I. Simms (2001), Technical Report SCI Publication P259: The Fire Resistance of Concrete Filled Tubes to Eurocode 4, Steel Construction Institute (SCI), UK.

H.C. Han, Y.G. Kim, S.J. Kang and S.M. Choi (2007), The first application of non-covered CFT columns in actual construction in Korea, *Korean Society of Steel Construction* (KSSC), **19**(2), 77-83, Korea.

H. Saito and K. Ikeda (2001), Fire resistance of concrete-filled steel tube columns with inner reinforcement, *J. Struct. Constr. Eng. (AIJ)*, **549**, 151-157.

ISO 834, International Organization for Standardization (1999), Fire-Resistance Tests- Elements of Building Construction, Switzerland.

J. Ding and Y.C. Wang (2008), Realistic modeling of thermal and structural behaviour of unprotected concrete filled tubular columns in fire, *J. Constr. Steel Res.*, **64,** Issue 10, 1086-1102.

J.L. Ryddy, J.P. Marlo, S.A. Ioannides and F. Alfawakiri (2003), Fire Resistance of Structural Steel Framing, Steel Design Guide No. 19, American Institute of Steel Construction, Inc., Chicago, Illinois, USA.

Jing Yin, Xiao-xiong Zha and Long-yuan Li (2006), Fire Resistance of Axially Loaded Concrete Filled Steel Tube Columns, *J. Constr Steel Res.*, **62**, Issue 7, 723-729.

K.H. Tan and C.Y. Tang (2004), Interaction Model for Unprotected Concrete Filled Steel Columns Under Standard Fire Conditions, *J. Struct. Eng., ASCE*, **130**, 9, 1405-1413.

Korean Agency for Technology and Standards (2005), KS F 2257-1: Methods of Fire Resistance Test for Elements of Building Construction- General Requirements, Korea.

L.H. Han (2001), Fire Performance of Concrete Filled Steel Tubular Beam-Columns, *J. Constr. Steel Res.*, **57**, Issue 6,. 697-711.

L.H. Han, X.L. Zhao, Y.F. Yang and J.B. Feng (2003a), Experimental Study and Calculation of Fire Resistance of Concrete-Filled Hollow Steel Columns, *J. Struct. Eng., ASCE,* **129**(3), 346-356.

L.H. Han, Y.F. Yang and L. Xu (2003b), An Experimental Study and Calculation on the Fire Resistance of Concrete-Filled SHS and RHS Columns, *J. Constr. Steel Res.,* **59**, Issue 4, pp. 427-452.

R. Bergmann, C. Matsui, C. Meinsma and D. Dutta (1995), Design Guide for Concrete-filled Hollow Section Columns under Static and Seismic Loading, Koln: CIDECT, Vzerlag T.U.V. Rheinland.

S.M. Choi, K.S. Chung and D.K. Kim (1998), A theoretical studyz on the fire-resisting characteristics of CFT long/short columns, *Architectural Ins. Kor. Con. Pro.*, **18**(2), 305-310, Korea.

S.M. Choi, K.S. Chung and D.K. Kim (2000), Suggestion of fire-resisting maximum strength formula for CFT columns under central axial load upon a fire, *Architectural Ins. Kor. J.*, **16**(6),13-20.

S.M. Choi, D.K. Kim and K.S. Chung (2000), Structural Characteristics of CFT Columns subject to Fire Loading and Axial Force, Associate for International Cooperation and Research in Steel-Concrete Composite

Structures(ASCCS), pp. 271-278.
S.M. Choi, I.S. Yang and J.A. Chung (2003), Composite structure with fire-resistance, *Kor. Society Steel Construction* J., **15**(2), 51-63, Korea.
S.M. Choi, D.K. Kim, J.H. Kim, K.S. Chung and S.H. Park (2005), Experimental Study on Fire Resistance of Concrete-filled Steel Tube Column under Constant Axial Loads, *Int.l Jouf Steel Struct*, **5**(4), 305-313.
S.M. Choi, S.H. Park, K.S. Chung and D.K. Kim (2006), Review of Material Properties for Predicting the Fire Resistance of Concrete-Filled Steel Square Tube Column using the Numerical Method, Associate for International Cooperation and Research in Steel-Concrete Composite Structures(ASCCS), pp. 909-919, China.
S.M. Choi, S.H. Park, J.Y. Ryoo and K.S. Chung (2007), A numerical analysis of the fire-resistance of CFT columns under central axial load, Proceeding of Korean Society of Steel Construction, pp. 312-318, Korea.
S.M. Choi, J.Y. Ryoo, S.H. Park, H.C. Han and B.Y. Min (2007), An experimental study on the fire-resistance of non-covered CFT columns, Proceeding of Korean Society of Steel Construction, pp. 558-563, Korea.
T.T. Lie and M. Chabot (1992), Experimental Studies on the Fire Resistance of Hollow Steel Columns Filled with Plain Concrete, Institute for Research in Construction, National Research Council Canada.
V.K.R. Kodur and T.T. Lie (1995), Fire Performance of Concrete-filled Hollow Steel Columns, *J. Fire Pro. Eng.*, **7**(3), 89-98.
V.K.R. Kodur and T.T. Lie (1996), Fire Resistance of Circular Steel Columns Filled with Fiber-Reinforced *Concrete, J. Struct. Eng., ASCE,* **122**(7), 776-782.
V.K.R. Kodur and T.T. Lie (1997), Evaluation of the Fire Resistance of Rectangular Steel Columns Filled with Fibre-reinforced Concrete, *Canadian J. Civil Eng.,* **24**(3), pp. 339-349.
V.K.R. Kodur (1998), Design Equations for Evaluation Fire Resistance of SFRC-Filled HSS Columns, *J. Struct. Eng., ASCE,* **124**(6), pp. 671-677.
V.K.R. Kodur (1999), Performance-based Fire Resistance Design of Concrete-Filled Steel Columns, *J. Constr. Steel Res.*, **51**, Issue 1, pp. 21-36.
V.K.R. Kodur (2005), Achieving Fire Resistance through Steel Concrete Composite Construction, *Structures Congress*'05, New York, April 21-23, pp. 1-6.
V.K.R. Kodur and J.C. Latour (2005), Experimental Studies on the Fire Resistance of Hollow Steel Columns Filled with High-Strength Concrete, Research Report, Institute for Research in Construction, Canada.
V.K.R. Kodur (2007), Guidelines for Fire Resistant Design of Concrete-Filled Steel HSS Columns – State-of-the-Art and Research Needs, *Int. J. Steel Struct.,* 7, pp. 173-182.
X.X. Zha (2003), FE Analysis of Fire Resistance of Concrete Filled CHS Columns, *J. Constr. Steel Res.*, **59**, Issue 6, 769-779.
Y. Sakumoto, T. Okada, M. Yoshida and S. Tasaka (1994), Fire Resistance of Concrete-Filled Fire Resistant Steel-Tube Columns, *J. Mater. Civil Eng*, **6**(2), 169-184.
Y.C. Wang (2000), A Simple Method for Calculating the Fire Resistance of Concrete-filled CHS Columns, *J. Constr. Steel Res.*, **54**, Issue 3, 365-386.
Y.C. Wang (2002), Steel and Composite Structures- Behaviour and Design for Fire Safety, Spon Press- Taylor & Francis Group.

CC